Journal of Basics and Applied Sciences Research (JOBASR)
ISSN (print): 3026-9091, ISSN (online): 1597-9962
Volume 3(4) July 2025
DOI: https://dx.doi.org/10.4314/jobasr.v3i4.26

The New Extended Exponential-Gamma (NEEG) Distribution: Properties and Applications to Infectious Disease Modelling

Samuel Adewale Aderoju[1, 2*], Ganiyat Monishola Salau[2], Bello Ishola Sanni[3], Adesina Dauda Adeshola[4], Abdulazeez Kayode Jimoh[5], Taofeek Olalekan Wahab[6] & Uchechukwu Kalu[7]

[1,2,3,4,5,6&7]Department of Mathematics and Statistics, Kwara State University, Malete, P.M.B. 1530, Ilorin, Nigeria.
[2]Statistics Program, BOWEN University, Iwo, Osun State, Nigeria
[*]Corresponding Author Email: samuel.aderoju@kwasu.edu.ng

ABSTRACT

This study introduces the New Extended Exponential-Gamma (NEEG) distribution, a flexible lifetime model developed to address the limitations of classical and generalized distributions in capturing real-world data complexity. The statistical properties of the proposed distribution are thoroughly explored, including its probability density function, cumulative distribution function, and parameter estimation via the maximum likelihood method. The practical effectiveness of the NEEG model is demonstrated using two real-life COVID-19 datasets from Italy and Nigeria, where it is benchmarked against several existing models such as the Gamma, Exponential, UYEG, and two variants of the Generalized Lindley distribution. Model comparison was conducted using a combination of information criteria (AIC, AICc, BIC, HQIC) and graphical tools such as density plots overlaid on empirical histograms. The results consistently show that the NEEG distribution provides the best fit across both datasets, outperforming all competing models in terms of flexibility, goodness-of-fit, and alignment with the empirical data. The model's adaptability to skewed and peaked data structures is particularly evident in pandemic-related scenarios, where traditional models often fail. These findings position the NEEG distribution as a powerful and versatile tool for statistical modelling in public health, reliability analysis, and other domains requiring robust handling of non-normal, skewed, or heavy-tailed data. Future research may extend the model into regression frameworks or multivariate contexts to enhance its applicability further.

Keywords:
New Extended Exponential-Gamma Distribution;
Flexible models;
Maximum likelihood Estimation; Survival Analysis; COVID-19 Data;
Skewed distributions

INTRODUCTION

One notable development in lifetime data modelling is the formulation of the Exponential-Gamma (EG) distribution, initially introduced by Lindley (1958) and Ogunwale et al. (2019). This model, which blends features of the Exponential and Gamma distributions, offers enhanced adaptability in characterizing lifetime data with variable hazard rates. Building on this innovation, Umar and Yahya (2021) proposed the New Exponential-Gamma distribution, incorporating special cases from the Exponential, Lindley, and their generalized forms (Gupta & Kundu, 2001; Nadarajah et al., 2011; Aderoju, 2021; Aderoju & Babaniyi, 2023; Suleman et al., 2025). These extensions significantly broadened the model's applicability, particularly in situations where hazard rates are not constant.

Broadly, in applied statistical modelling across disciplines like health sciences, reliability engineering, economics, climate studies, and more, the need for highly flexible distributions has prompted researchers to introduce new models via parameterization and distribution compounding. These models often outperform classical ones due to their ability to capture complex patterns and tail behaviors. Examples of recent generalizations include the Gumbel-based T-X model by Fayomi et al. (2024), the Modified Frechet–Rayleigh Distribution by Muhammad et al. (2022), and the Exponential Transformed Inverse Rayleigh distribution by Proloy & Shreya (2022). Aderoju (2021) introduced the Samade distribution, a mixture of exponential and gamma distributions, deriving its mathematical properties and demonstrating its improved fit for lifetime data compared to existing models.

How to cite this article: Samuel A. A., Ganiyat M. S., Bello I. S., Adesina D. A., Abdulazeez K. J., Taofeek O. W. & Uchechukwu K. (2025). The New Extended Exponential-Gamma (NEEG) Distribution: Properties and Applications to Infectious Disease Modelling. *Journal of Basics and Applied Sciences Research*, *3*(4), 225-235. https://dx.doi.org/10.4314/jobasr.v3i4.26

The Samade distribution encompasses moments, reliability functions, and entropy measures, and has been shown to outperform classical models on various datasets. Building on the Samade distribution, Aderoju and Babaniyi (2023) developed the Power Samade distribution, a three-parameter lifetime model that generalizes the gamma family. This distribution provides additional flexibility in modelling the shape of the density and hazard rate functions, and its efficacy has been validated using real datasets, where it outperformed the exponential, Lindley, and other related distributions in terms of AIC and BIC.

Additional works by Albalawi et al. (2022), Abiodun & Ishaq (2022), Idika et al. (2021), Ibeh et al. (2021), Aderoju & Adeniyi (2022), and Elangovan et al. (2023) demonstrate the growing trend of constructing new distribution families tailored to specific data characteristics.

Against this backdrop, Aderoju (2021) and Aderoju & Jolayemi (2022) advanced the lifetime model by embedding it within a new family of Exponential-Gamma distribution.

Aderoju and Jolayemi (2022) proposed the Power Hamza distribution, which generalizes the Hamza distribution and offers greater flexibility for survival time analysis. This model has been applied successfully to survival data, providing better fits than classical models.

In further work, Aleshinloye et al. (2023) developed and applied generalized gamma-Weibull and other related distributions for modelling cancer data and other lifetime data sets, again demonstrating improved flexibility and fit over traditional models.

The exponential-gamma distribution and its generalizations, including those proposed by Aderoju, have found extensive application in fields where accurate modelling of lifetime and failure data is critical. In biostatistics, these models have been used to analyze survival times and remission periods in clinical studies, often providing a superior fit compared to traditional exponential or gamma models (Aderoju et al., 2023; Alnaji and Alghamdi, 2023). In reliability engineering, the distributions are particularly useful for systems with non-constant or bathtub-shaped hazard rates, allowing for more accurate estimation of failure probabilities and system reliability (Thomas & Chacko, 2022).

Comparative analyses have consistently shown that the exponential-gamma distribution and its extensions outperform classical models such as the Weibull, Erlang, and generalized extreme value distributions, particularly when modelling data with non-monotonic hazard functions (Alnaji and Alghamdi, 2023 and Wang et al., 2024).

Empirical comparisons have shown that the New Exponential-Gamma distribution frequently provides superior fits to real-world data when compared with the classical Exponential model and its extensions. Nevertheless, existing models still exhibit limitations, especially in capturing intricate hazard rate behaviors such as non-monotonicity and bathtub patterns.

To address this gap, this study proposes a more generalized form known as the New Extended Exponential-Gamma (NEEG) distribution. The NEEG distribution is constructed by compounding the Exponential distribution with the Gamma distribution using transformed mean proportion. The main objective of this research is to investigate the mathematical properties of the NEEG distribution, examine its submodels, and evaluate its performance using real datasets. The proposed model will be compared with several well-known lifetime distributions to highlight its advantages in practical settings. Ultimately, the study contributes to the evolving framework of robust and flexible lifetime models.

The rest of the paper is organized as follows: Section 2 introduces the NEEG distribution**.** Section 3 outlines the estimation of its key statistical properties. In Section 4**,** a comprehensive maximum likelihood estimation of the parameters is conducted to evaluate. Section 5 contains applications to real-life datasets to demonstrate the practical utility of the model. The paper concludes with a summary and final observations in Section 6**.**

MATERIALS AND METHODS

The modified Lifetime distribution, named New Extended Exponential-Gamma (NEEG) distribution, is characterized by the parameters τ and ω, which are defined through its probability density function (pdf). This pdf follows the general structure of a k-component additive mixture distribution, as outlined by Everitt and Hand (1981). Specifically, for a random variable r, the pdf is given by:

$$f(z, \Theta) = \sum_{j=1}^{k} \pi_{j,} h_j(z, \Theta_j) \, , \qquad (1)$$

where Θ_j is the vector of parameters for the mixture models, π_j is the mixture proportion and $\sum_{j=1}^{k} \pi_j = 1$.

Note that the pdf (1) can be shown as a mixture of $Exponential\ (\tau)$ and $Gamma\ (\tau, \omega)$ distributions as follows:

$$f(z; \tau, \omega) = \pi h_1(z; \tau) + (1 - \pi) h_2(z; \tau, \omega) \, , \qquad (2)$$

where

$\pi = \frac{\Gamma(\tau)}{1+\Gamma(\tau)}$, is the mixing proportion (or mixture weight), which is obtained as the proportion of the first moments of h_1 and h_2.

Exponential Distribution

$$h_1(r;\tau,\omega) = \tau x^{\tau-1} e^{-\tau x}\,, \quad x > 0 \qquad (3)$$

and

Gamma Distribution

$$g_1(x;\tau,\omega) = \frac{\omega^{\tau}}{\Gamma(\tau)} x^{\tau-1} e^{-\omega x}\,, \quad x > 0 \qquad (4)$$

where:

1. $\tau > 0$ is the shape parameter.
2. $\omega > 0$ is the scale parameter.

Now substituting (3) and (4) into (2), we have

$$f(z;\tau,\omega\,) = \frac{\Gamma(\tau)}{1+\Gamma(\tau)}\left(\tau e^{-\tau x}\right) + \left(1 - \frac{\Gamma(\tau)}{1+\Gamma(\tau)}\right)\frac{\omega^{r} r^{\omega-1}}{\Gamma(\tau)} e^{-\omega r}$$

Therefore,

$$f(z;\tau,\omega) = \frac{\omega + z^{\tau-1}\omega^{\tau}}{1+\Gamma(\tau)} e^{-\omega z}$$

The corresponding cumulative distribution function (cdf) is

$$F(z;\tau,\omega) = \int_0^z f(t;\tau,\omega,)dt$$

$$F(z;\tau,\omega) = \int_0^z \frac{(\omega + t^{\tau-1}\omega^{\tau})}{(1+\Gamma(\tau))} e^{-\omega t} dt$$

$$= \frac{1 - e^{-x\omega} + (\Gamma(\tau) - \Gamma(\tau, z\omega))}{1+\Gamma(\tau)}$$

$$\therefore F(z;\tau,\omega\,) = \frac{1 - e^{-z\omega} + (\Gamma(\tau) - \Gamma(\tau, z\omega))}{1+\Gamma(\tau)}$$

RESULTS AND DISCUSSION

Figure 1 presents the pdf plots of the NEEG distribution at varying values of the parameters. This visual exploration confirms the proposed model's parametric versatility, capturing various real-world data patterns, from sharp, peaked distributions to long-tailed, skewed scenarios. Such adaptability makes it well suited for complex lifetime, biomedical, or reliability datasets where classical distributions often fail. In panel (a): $\hat{\tau} = 0.25$, the density is highly right-skewed, peaking sharply near zero and decaying rapidly. As $\widehat{\omega}$ increases, the distribution flattens and spreads slightly, indicating greater dispersion. This reflects the model's ability to capture heavy-tailed behaviours for small $\hat{\tau}$. In panel (b): $\hat{\tau} = 5$, a pronounced mode emerges, and the curves shift rightward with increasing $\widehat{\omega}$. The distribution gains flexible peakedness, useful for modelling moderate survival times. In panel (c): $\hat{\tau} = 10$, the effect of $\widehat{\omega}$ becomes even clearer: smaller $\widehat{\omega}$ yields sharper peaks, while larger $\widehat{\omega}$ induces heavier tails.Demonstrates the distribution's capacity to adjust kurtosis and skewness simultaneously. In panel (d): $\hat{\tau} = 10$, with a higher $\hat{\tau}$, the distribution shifts substantially to the right and remains unimodal. Increasing $\widehat{\omega}$ maintains a sharp mode but controls tail length, indicating robust tail adaptability.

Moreover, Figure 2 represents two panels that display cdf plots for a NEEG distribution under various combinations of the parameters. The plots illustrate how changes in these parameters influence the rate of accumulation of probability density. In the left panel $(\hat{\tau} = 10)$, as $\widehat{\omega}$ increases from 0.25 to 2.50: the cdf rises more steeply, indicating a faster accumulation of probability. The distribution becomes more concentrated near smaller values of z. This implies that higher $\widehat{\omega}$ leads to lower median and shorter tails, highlighting the distribution's ability to model early-event or short-time phenomena effectively. In the right panel $(\hat{\tau} = 10)$, all curves rise quickly, but the speed and steepness still vary with $\widehat{\omega}$. The curve for $\widehat{\omega} = 2.5$approaches 1 much faster than that for $\widehat{\omega} = 0.25$. These plots validate the distribution's flexible cumulative behaviour, capable of capturing both rapid and gradual event accumulation patterns. This makes the model suitable for diverse applications such as failure time analysis, risk modelling, and biomedical event studies, where classical models may not offer this dual sensitivity to both early and late event probabilities.

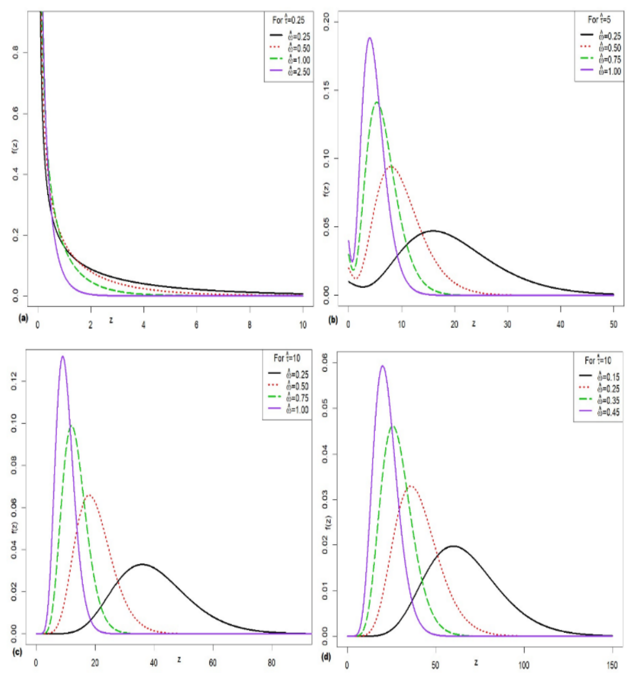

Figure 1: Visualization of the NEEG distribution's pdf across different τ and ω parameter settings

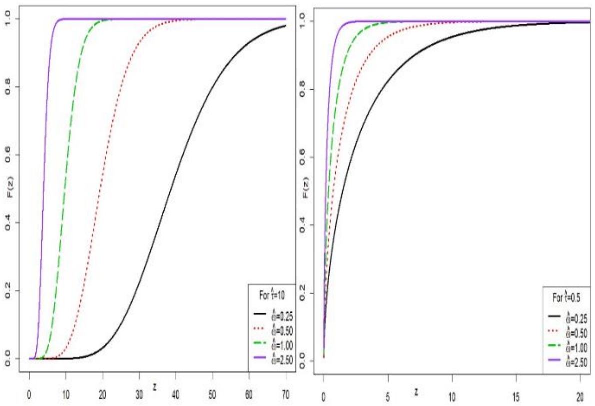

Figure 2:Visualization of the NEEG distribution's cdf across different τ and ω parameter settings

STATISTICAL PROPERTIES

In this section, we explore various statistical properties of the $NEEG(\tau,\omega)$ distribution, including its moments, measures of skewness and kurtosis, the moment generating function, as well as the quantile function, median, and entropy.

Moments

The first four raw moments of the proposed probability density function $f(z;\tau,\omega)$ are obtained as follows:

Let

$$\mu_r = \mathrm{E}(z^r) = \int_0^\infty z^r f(z;\tau,\omega)dx$$

$$\mu_r = \int_0^\infty z^r \frac{(\omega + z^{\tau-1}\omega^\tau)}{(1+\Gamma(\tau))} e^{-\omega z} dz$$

$$= \frac{\omega^{-r}(\Gamma(1+r)+\Gamma(r+\tau))}{1+\Gamma(\tau)}$$

Therefore, when $r = 1,2,3,4$ we have:

$$\mu_1 = \frac{1+\Gamma(1+\tau)}{\omega+\omega\Gamma(\tau)}$$

$$\mu_2 = \frac{2+\Gamma(2+\tau)}{\omega^2(1+\Gamma(\tau))}$$

$$\mu_3 = \frac{6+\Gamma(3+\tau)}{\omega^3(1+\Gamma(\tau))}$$

$$\mu_4 = \frac{24+\Gamma(4+\tau)}{\omega^4(1+\Gamma(\tau))}$$

Hence the variance (σ^2) is

$$Var(x) = \sigma^2 = \frac{(1+\Gamma(1+\tau))^2}{(\omega+\omega\Gamma(\tau))^2} + \frac{2+\Gamma(2+\tau)}{\omega^2(1+\Gamma(\tau))}$$

While the coefficient of variation (CV) is

$$CV = \frac{\sqrt{(1-2\Gamma(1+\tau)-\Gamma(1+\tau)^2+\Gamma(2+\tau)+\Gamma(\tau)(2+\Gamma(2+\tau))))}}{(\omega(1+\Gamma(\tau))(1+\Gamma(1+\tau))}$$

The skewness and the kurtosis were also obtained, respectively, as:

$$S_k = \frac{(6+\Gamma(3+\tau))}{\omega^3(1+\Gamma(\tau))(-\frac{(1+\Gamma(1+\tau))^2}{(\omega+\omega\Gamma(\tau))^2}+\frac{2+\Gamma(2+\tau)}{\omega^2(1+\Gamma(\tau))})^{3/2}}$$

and

$$K_s = \frac{((1+\Gamma(\tau))^3(24+\Gamma(4+\tau)))}{(1-2\Gamma(1+\tau)-\Gamma(1+\tau)^2+\Gamma(2+\tau)+\Gamma(\tau)(2+\Gamma(2+\tau)))^2}$$

Moment Generating Function

The moment generating function (mgf) plays a fundamental role in probability theory, offering a compact representation of a random variable's distribution. By encoding all the moments in a single function, the MGF provides a powerful tool for analyzing distributional properties, deriving moments, and facilitating comparisons between models. In this section, we derive the MGF of the NEEG distribution as follows.

$$M_X(\mathrm{t}) = \mathrm{E}(e^{tz}) = \int_0^\infty e^{tz} f(z;\tau,\omega)dx$$

$$M_X(\mathrm{t}) = \int_0^\infty e^{tz} \frac{(\omega + z^{\tau-1}\omega^\tau)}{(1+\Gamma(\tau))} e^{-\omega z} dx$$

$$M_X(\mathrm{t}) = \frac{1}{1+\Gamma(\tau)}\left(\frac{\omega}{\omega-t} + \frac{\omega^\tau\Gamma(\tau)}{(\omega-t)^\tau}\right)$$

Quantile and Median

Given the pdf and cdf in equations (1) and (2), respectively, the quantile function (inverse of cdf) was obtained as

$$F(x_p) = p \quad for\ x_p, \quad where\ 0 \le p \le 1.$$

$$x_p = F^{-1}(p)$$

Therefore,

$$\frac{1-e^{-x\omega}+\Gamma(\tau)-\Gamma(\tau,z\omega))}{1+\Gamma(\tau)} = p$$

$$1-e^{-x\omega}+\big(\Gamma(\tau)-\Gamma(\tau,z\omega)\big) = p\big(1+\Gamma(\tau)\big) \qquad (5)$$

This equation does **not** have a closed-form solution in general, but we can express the quantile function in terms of the inverse of the incomplete gamma function:

$x_p = F^{-1}(p)$ is the solution to (5)

The median is 50th percentile ($p = 0.5$)

$$1-e^{-z_{0.5}\omega}+(\Gamma(\tau)-\Gamma(\tau,z_{0.5}\omega)) = 0.5(1+\Gamma(\tau))$$

Similarly, this requires numerical methods to solve for $z_{o.5}$.
For $\tau = 1$, the median simplifies to:

$$z_{o.5} = \frac{\ln(2)}{\omega}$$

Figure 3 represents a quantile function plot. The quantile function of the new Exponential-Gamma distribution displayed here confirms it is a right-skewed, positively biased, and flexible continuous distribution, suitable for modelling asymmetric data with moderate to heavy tails. The visualization aids in understanding the distribution's behavior, especially in assessing spread and the impact of parameter changes on percentiles.

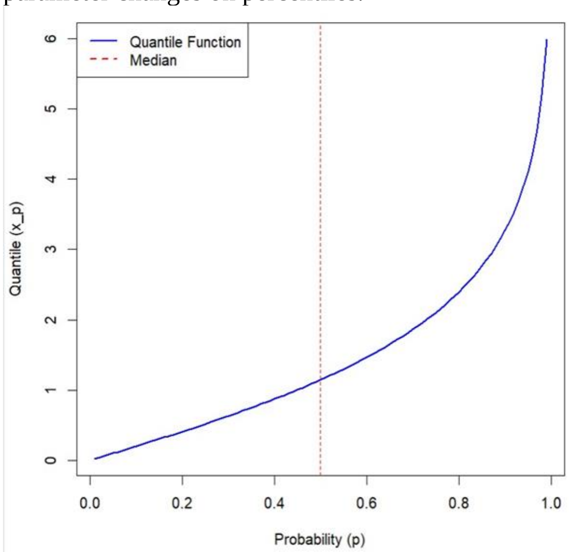

Figure 3: The **Quantile Function Plot**

Rényi's Entropy

Rényi's entropy is particularly useful for analyzing the diversity and complexity of probability distributions. In this section, we derive the Rényi entropy of the NEEG model to assess its information-theoretic characteristics and capture the degree of randomness inherent in the distribution. The entropy is:

$$H_\alpha(Z) = \frac{1}{1-\alpha}\log\left[\int_0^\infty f(z;\tau,\omega)^\alpha \, dz\right]$$

$$H_\alpha(Z) = \frac{1}{1-\alpha}\log\left[\left(\frac{1}{1+\Gamma(\tau)}\right)^\alpha \int_0^\infty (\omega + z^{\tau-1}\omega^\tau)^\alpha e^{-\omega z\alpha} \, dz\right]$$

We use the binomial series expansion to get:

$$H_\alpha(Z) = \frac{1}{1-\alpha}\log\left[\frac{\omega^{\alpha-1}}{(1+\Gamma(\tau))^\alpha}\sum_k^\infty \binom{\alpha}{k}\frac{\Gamma(k(\tau-1)+1)}{(\alpha)^{k(\tau-1)+1}}\right],$$

when $\alpha > 0$

Order Statistics

Order statistics serve as a foundational approach in drawing inferences from reliability data. Given independent and identically distributed random variables $X_1, X_2, \ldots, X_n$ following the NEEG distribution, the smallest and largest observations in the sample are referred to as the minimum and maximum order statistics, respectively. These are defined as $X_{(1)} = \min(X_1, X_2, \ldots, X_n)$ and $X_{(n)} = \max(X_1, X_2, \ldots, X_n)$The complete set of ordered values satisfies $X_{(1)} \le X_{(2)} \le \ldots \le X_{(n)}$. The pdf of the kth order statistic, denoted $X_{(k)}$, is given by:

$$f_{z(k)}(z|\tau,\omega) = \frac{n!}{(k-1)!\,(n-k)!} f(z)[F(z)]^{k-1}[1-F(z)]^{n-k}$$

From (5), we can write:

$$f_{z(k)}(z|\tau,\omega) = \frac{n!}{(k-1)!\,(n-k)!}\frac{(\omega + z^{\tau-1}\omega^\tau)e^{-\omega z}}{(1+\Gamma(\tau))}\left[\frac{1-e^{-z\omega}+\left(\Gamma(\tau)-\Gamma(\tau,z\omega)\right)}{1+\Gamma(\tau)}\right]^{k-1} \times \left[\frac{e^{-z\omega}+\Gamma(\tau,z\omega)}{1+\Gamma(\tau)}\right]^{n-k}$$

The functions of the first and n*th* order statistics, respectively, are:

$$f_{z(1)}(z|\tau,\omega) = \frac{n!}{(k-1)!\,(n-k)!}\frac{(\omega + z^{\tau-1}\omega^\tau)e^{-\omega z}}{(1+\Gamma(\tau))}\left[\frac{e^{-z\omega}+\Gamma(\tau,z\omega)}{1+\Gamma(\tau)}\right]^{n-1}$$

and

$$f_{z(n)}(z|\tau,\omega) = \frac{n!}{(k-1)!\,(n-k)!}\frac{(\omega + z^{\tau-1}\omega^\tau)e^{-\omega z}}{(1+\Gamma(\tau))}\left[\frac{1-e^{-z\omega}+(\Gamma(\tau)-\Gamma(\tau,z\omega))}{1+\Gamma(\tau)}\right]^{k-1}$$

Survival Function

Let z be a continuous random variable with cdf $F(z;\tau,\omega)$. The **survival function**, which represents the probability that the event of interest has not occurred by time z, is defined as:

$$S(z;\tau,\omega) = 1 - F(z;\tau,\omega)$$

$$S(z;\tau,\omega) = 1 - \frac{1-e^{-z\omega}+(\Gamma(\tau)-\Gamma(\tau,z\omega))}{1+\Gamma(\tau)}$$

$$S(z;\tau,\omega) = \frac{e^{-z\omega}+\Gamma(\tau,z\omega)}{1+\Gamma(\tau)}$$

Hazard Function

Let z be a continuous random variable characterized by the probability density function $f(z;\tau,\omega)$ and the cumulative distribution function $F(z;\tau,\omega)$. The hazard rate function, also referred to as the failure rate function, is given by:

$$h(z)=\frac{f(z;\tau,\omega)}{1-F(z;\tau,\omega)}$$
$$h(z)=\frac{z\omega+z^{\tau}\omega^{\tau}}{z+e^{z\omega}z\Gamma(\tau,z\omega)}$$
$$h(z)=\frac{\omega+z^{\tau-1}\omega^{\tau}}{(1+e^{z\omega}\Gamma(\tau,z\omega))}$$

Figure 5 represents the hazard function plots, which demonstrate the flexibility of the hazard function for the parameters$\hat{\tau}$ and $\hat{\omega}$. For high $\hat{\tau}$ (a), the hazard increases (aging systems).For low $\hat{\tau}$ (b), the hazard decreases (infant mortality systems). This behavior is desirable in modelling real-world data with varying failure dynamics, including increasing, decreasing, or non-monotonic hazard rates. These plots show that the NEEG distribution can model diverse lifetime behaviors depending on parameter choices. This adaptability makes it valuable in reliability analysis, biomedical studies, and engineering applications, where different types of failure risks exist.

Figure 6 represents the survival function plots, which are monotonically decreasing in all cases. For higher $\hat{\tau}$ or lower $\hat{\tau}$, the survival probability decreases more rapidly, indicating higher risk or shorter time to failure. This is useful in reliability analysis, biomedical survival analysis, and epidemiological modelling. These plots demonstrate the flexibility of the NEEG distribution to model systems with different failure behaviors, from quick failure to long-term survival.

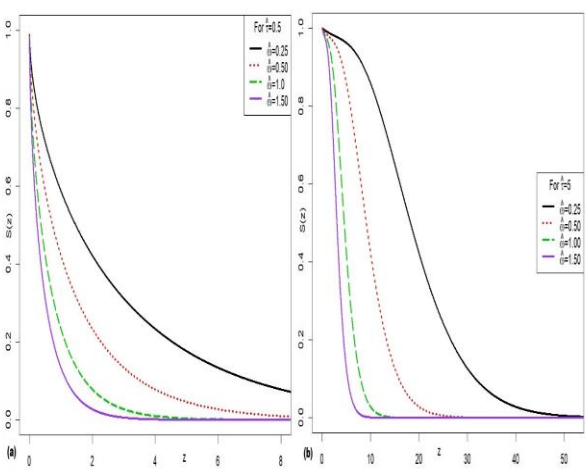

Figure 4: Survival function plots

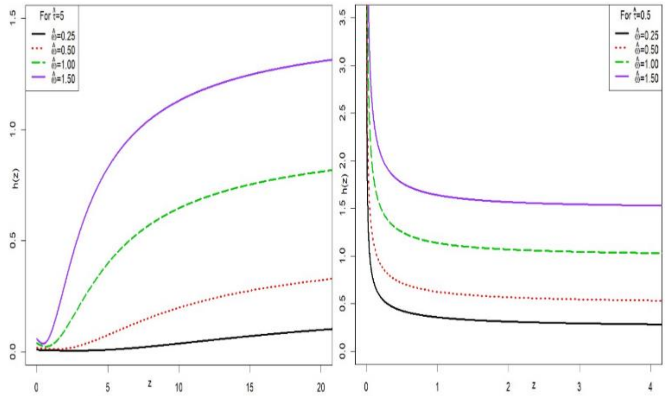

Figure 5: hazard plot

MAXIMUM LIKELIHOOD ESTIMATION

Let $X_1, X_2, X_3, \dots, X_n$ is a random sample of size *n* from the NEEG distribution, the maximum likelihood function of the parameters can be written as

$$L(\tau,\omega)=\prod_{i=1}^{n} f(z_i;\ \tau,\omega),$$
$$L(\tau,\omega)=\prod_{i=1}^{n}\frac{(\omega+z_i^{\tau-1}\omega^{\tau})}{(1+\Gamma(\tau))}e^{-\omega z_i},$$

and the log-likelihood function is

$$\ell(\tau,\omega)=\sum_{i=1}^{n} ln f(z_i;\ \tau,\omega)$$
$$\ell(\tau,\omega)=\sum_{i=1}^{n}[-\omega z_i+\ln(z_i\omega+z_i^{\tau-1}\omega^{\tau})]-ln z_i - ln(1+\Gamma(\tau))$$
$$\ell(\tau,\omega)=-\omega\sum_{i-1}^{n} z_i+\sum_{i=1}^{n}\ln(z_i\omega+z_i^{\tau-1}\omega^{\tau})] - \sum_{i=1}^{n} ln z_i - n ln(1+\Gamma(\tau))$$

Differentiating the $\ell(\tau,\omega)$ partially with respect to the associated parameters, we have

$$\frac{\partial\ell(\tau,\omega)}{\partial\tau}=\sum_{i=1}^{n}\frac{z_i^{\tau}\omega^{\tau}\ln(z_i\omega)}{z_i\omega+z_i^{\tau}\omega^{\tau}}-n\frac{\Gamma'(\tau)}{1+\Gamma(\tau)} = 0 \qquad (7)$$

$$\frac{\partial\ell(\tau,\omega)}{\partial\omega}=-\sum_{i-1}^{n} z_i+\sum_{i=1}^{n}\frac{z_i\omega+\tau z_i^{\tau}\omega^{\tau-1}}{z_i\omega+z_i^{\tau}\omega^{\tau}} = 0\,, \qquad (8)$$

where$\Gamma'(\tau)$ is the digamma function.

The Maximum Likelihood Estimates (MLEs), $\hat{\tau}$ *and* $\hat{\omega}$, of τ and ω are solutions of equations (7) and (8). Analytical expressions for $\hat{\tau}$ *and* $\hat{\omega}$ are not available. Hence, we computed the MLEs numerically using the *nloptr* package and *bobyqa* function in R software (R Core Team, 2025)

Simulation Study

In this subsection, we examine the performance of the maximum likelihood estimators $\hat{\tau}_{MLE}$ and $\widehat{\omega}_{MLE}$ for the NEEG distribution using a comprehensive simulation framework. The procedure involves generating synthetic data based on the inverse cumulative distribution function, repeated over 1,000 iterations for varying sample sizes $n = 50, 100, \dots, 1000$, The simulation study is conducted for three parameter settings: τ = 5, ω = 5; τ = 0.5, ω = 5 and τ = 0.5, ω = 0.5. To assess the quality of the estimators, we employ two key performance metrics: bias and mean squared error (MSE), defined mathematically as follows.

$$MSE(\widehat{\omega}_{MLE}) = \frac{1}{N}\sum_{i=1}^{N}(\hat{\tau}_i - \tau)^2$$

and

$$Bias(\widehat{\omega}_{MLE}) = \frac{1}{N}\sum_{i=1}^{N}(\hat{\tau}_i - \tau\ )$$

The numerical outcomes of the simulation are displayed in Table 1. Based on the simulation findings for the NEEG distribution, a consistent pattern emerges as the sample size n increases (i.e., as $n \to \infty$), both $\hat{\tau}_{MLE}$ and $\widehat{\omega}_{MLE}$ increasingly approximate their true parameter values, suggesting estimator consistency. Furthermore, the corresponding mean squared errors (MSEs) and biases of these estimators steadily decline toward zero, reflecting improved accuracy and reduced estimation error with larger samples.

Table 1: The numerical illustration of the Simulation Study of the NEEG distribution

	n	Parameters	MLEs	Biases	MSEs
τ = 5 ω = 5	50	τ ω	5.4085 5.4431	0.4085 0.4431	0.6591 0.7568
	150	τ ω	4.9733 4.9256	-0.0267 -0.0744	0.0538 0.1289
	300	τ ω	4.9818 4.9693	-0.0182 -0.0307	0.0268 0.0317
	500	τ ω	5.0667 5.0998	0.0667 0.0998	0.0429 0.0776
	750	τ ω	5.0052 4.9756	0.0052 -0.0244	0.0106 0.0117
	1000	τ ω	5.0039 4.9707	0.0039 -0.0293	0.0117 0.0173
τ = 0.5 ω = 5	50	τ ω	0.4632 4.9779	-0.0368 -0.0221	0.0132 1.7141
	150	τ ω	0.4593 4.7389	-0.0407 -0.2611	0.0055 0.3599
	300	τ ω	0.4493 4.6210	-0.0507 -0.3790	0.0046 0.3443
	500	τ ω	0.4714 4.6647	-0.0286 -0.3353	0.0019 0.2105
	750	τ ω	0.4645 4.7577	-0.0355 -0.2423	0.0024 0.1584
	1000	τ ω	0.4508 4.8558	-0.0492 -0.1442	0.0028 0.0898
τ = 0.5 ω = 0.5	50	τ ω	0.5354 0.5435	0.0354 0.0435	0.0098 0.0057
	150	τ ω	0.5069 0.5259	0.0069 0.0259	0.0042 0.0021
	300	τ ω	0.5093 0.5223	0.0093 0.0223	0.0031 0.0013
	500	τ ω	0.4899 0.5114	-0.0101 0.0114	0.0008 0.0005
	750	τ ω	0.4974 0.5075	-0.0026 0.0075	0.0004 0.0002
	1000	τ ω	0.4983 0.5025	-0.0017 0.0025	0.0003 0.0000

REAL DATA APPLICATION

This section assesses the performance of the newly introduced NEEG distribution by applying it to two real-life datasets. For comparative purposes, the Gamma, exponential, exponential-gamma distribution (UYEG) introduced by Umar and Yahya (2021), the generalized Lindley distribution (Nadarajah_GLD) introduced by Nadarajah et al. (2011), and the New generalized two-parameter Lindley distribution (Ekhosuehi_GLD) introduced by Ekhosuehi et al. (2018), are also fitted to the same datasets. Parameter estimation is carried out using R software to ensure precise and reliable results.

Dataset 1: This was originally analyzed by Qayoom et al. (2025) and consists of the ratio between daily new deaths and daily new cases of COVID-19 in Italy recorded for 111 days from 1 April to 20 July 2020.

Dataset 2: This dataset represents the time-to-recovery (in days) of COVID-19 patients at Lagos state, Nigeria, in 2020 (Aderoju et al., 2025). It comprises 553 patients.

Table 2: Estimation of distribution parameters and Distribution performance using information criterion values based on given COVID-19 datasets.

Dataset 1: COVID-19 in Italy recorded for 111 days from 1 April to 20 July 2020 (Qayoom et al., 2025)						
	MLEs (S.E.s)					
Model	$\hat{\tau}$	$\hat{\omega}$	**AIC**	**AICc**	**BIC**	**HQIC**
NEEG	4.9108 (0.3399)	28.4381 (2.5472)	-250.3052	-250.1941	-244.8862	-248.1069
Gamma	3.8492 (0.4959)	23.0778 (3.176)	-248.7172	-248.6061	-243.2981	-246.5188
Nadarajah_GLD	4.2962 (0.6896)	13.5483 (1.1298)	-244.1625	-244.0514	-238.7435	-241.9642
Ekhosuehi_GLD	1.5195 (0.3244)	6.3784 (0.6253)	-174.8544	-174.7433	-169.4354	-172.6561
UYEG	1.5214 (0.3676)	6.3438 (0.6319)	-174.5108	-174.3997	-169.0918	-172.3125
Exp.	-	5.9955 (0.5691)	-173.6027	-173.566	-170.8931	-172.5035
Dataset 2: Covid-19 data in Nigeria (Lagos data) Aderoju et al. (2025)						
NEEG	4.7561 (0.136)	0.4438 (0.0167)	3309.437	3309.459	3318.068	3312.809
UYEG	4.3694 (0.1727)	0.4129 (0.0195)	3315.033	3315.055	3323.664	3318.405
Gamma	3.4554 (0.1986)	0.3386 (0.0209)	3342.082	3342.104	3350.713	3345.454
Nadarajah_GLD	2.2552 (0.1574)	0.2595 (0.0094)	3342.292	3342.313	3350.922	3345.664
Ekhosuehi_GLD	3.6345 (0.2592)	0.3100 (0.0216)	3407.531	3407.553	3416.162	3410.903
Exp.	-	0.098 (0.0042)	3677.031	3677.039	3681.347	3678.717

Table 2 presents the parameter estimates, standard errors, and model selection criteria reported. This provides compelling evidence of the superiority of the proposed NEEG distribution in modelling Infectious Disease.

For the Italy dataset (Dataset 1), the NEEG distribution yielded the lowest values across all evaluated information criteria (AIC, AICc, BIC, and HQIC), indicating a superior fit compared to the Gamma, UYEG, and other generalized Lindley-type models. Notably, the NEEG model attained a significantly lower AIC (−250.31) than the Gamma (−248.72) and Nadarajah_GLD (−244.16), reinforcing its improved flexibility in modelling real-life data with skewness and heavy tails. Furthermore, the associated standard errors of the MLEs are acceptably small, suggesting stable and reliable parameter estimates.

In the case of the Lagos dataset (Dataset 2), the trend remained consistent. The NEEG distribution again outperformed all competing models with the lowest AIC (3309.44) and other model selection criteria. Although UYEG and Gamma models were fairly competitive in terms of fit, they were still outmatched by NEEG in both numerical efficiency and graphical smoothness. The exponential distribution consistently lagged across both datasets, confirming its limited capacity for capturing complex real-world variations.

Figures 6 and 7 further substantiate these findings through graphical density comparisons. In both figures, the NEEG curve aligns closely with the shape of the empirical histogram, particularly around the mode and tails. Competing models such as the Ekhosuehi_GLD and Exponential either under-fit or over-smooth portions of the data, resulting in noticeable deviation from the empirical distribution. The NEEG model, by contrast, strikes an effective balance between flexibility and smoothness, offering a better approximation of the observed distributions. Overall, both the statistical indicators and visual diagnostics affirm the NEEG model's capacity to accurately capture the underlying structure of pandemic-related datasets, thus making it a compelling alternative to existing flexible distributions.

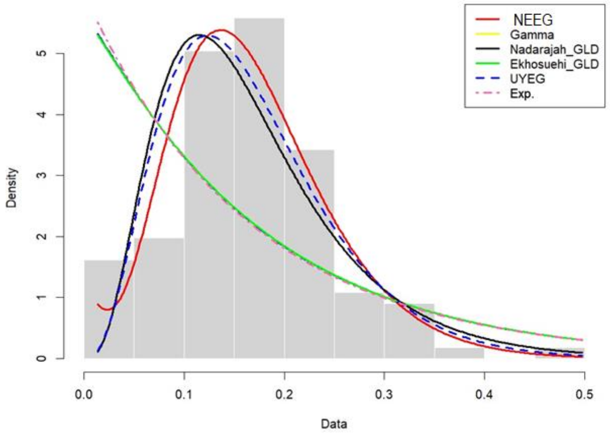

Figure 6: Italy data fitness plots

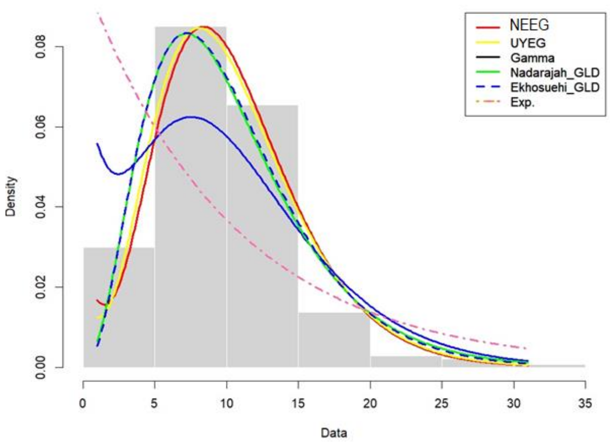

Figure 7: Lagos data fitness plots

CONCLUSION

This study introduces the NEEG distribution as a novel extension for modelling lifetime and survival data. Key distributional characteristics and statistical properties such as the probability density function, moments, the mean and variance, survival function, hazard rate function, moment generating function, order statistics, and Rényi's Entropy have been discussed. The parameters of the proposed new distribution are estimated by using the method of maximum likelihood estimation. Finally, the robustness of the model was assessed using two real-life COVID-19 datasets: one from Italy and another from Lagos, Nigeria. To evaluate its practical usefulness, the NEEG distribution was fitted to both datasets alongside well-established models such as the Gamma, Exponential, UYEG, and two generalized Lindley distributions (Nadarajah_GLD and Ekhosuehi_GLD). Parameter estimation was conducted via the maximum likelihood approach using R software. Model performance was benchmarked using a suite of information criteria, including AIC, AICc, BIC, and HQIC. Additionally, visual fit diagnostics through histogram-based density overlays were employed to complement the quantitative comparison. Findings from both datasets reveal that the NEEG distribution consistently offers a superior fit, capturing complex data behavior such as skewness and kurtosis more effectively than its counterparts do. Particularly, the NEEG model demonstrated lower information criteria values and better graphical adherence to observed data patterns, while classical models like the Exponential distribution failed to capture the tail behavior adequately. The promising performance of the NEEG model across different datasets underscores its potential as a versatile tool for analyzing real-world biomedical and epidemiological data. Given its flexibility and fit precision, the NEEG distribution may find application in broader domains such as reliability analysis, public health forecasting, and risk modelling. Future extensions could explore Bayesian estimation frameworks or multivariate generalizations of the model to further enhance its adaptability and inferential power.

REFERENCE

Abiodun, A. A., & Ishaq, A. I. (2022). On Maxwell–Lomax distribution: Properties and applications. *Arab Journal of Basic and Applied Sciences*, 29(1), 221–232. https://doi.org/10.1080/25765299.2022.2093033

Aderoju, S. A., Dauda, K. A., & Olaifa, J. B. (2025). Development of new flexible lifetime model: Its associated inferences and applications to cancer and COVID-19 data. *Journal of Science and Technology*. 30(8). 13-27. https://doi.org/10.20428/jst.v30i8.3024

Aderoju, S. A., Aleshinloye, N. I., Taiwo, B. L., & Sanni, B. I. (2023). A new lifetime distribution and its application to cancer data. *Journal of Biostatistics and Epidemiology*, 9(4), 451–460. https://doi.org/10.18502/jbe.v9i4.16670

Aderoju, S. A., & Babaniyi, O. (2023). Power Samade distribution: Its properties and application to real lifetime data. *Nigerian Journal of Science and Environment*, 21(1), 237–248.

Aderoju, S. A., & Jolayemi, E. T. (2022). Power Hamza distribution and its applications to model survival time. *Journal of the Nigerian Statistical Association*, 34(1), 1–10.

Aderoju, S. A. (2021). Samade probability distribution: Its properties and application to real lifetime data. *Asian Journal of Probability and Statistics*, 14(1), 1–11. https://doi.org/10.9734/ajpas/2021/v14i130317

Aderoju, S. A., & Adeniyi, I. (2022). On Power Generalized Akash distribution with properties and applications. *Journal of Statistical Modelling & Analytics*, 4(1), 1–13.

Albalawi, O., Kabdwal, N. C., Azhad, Q. J., Hora, R., & Alsaedi, B. S. O. (2022). Estimation of the generalized logarithmic transformation exponential distribution under progressively Type-II censored data with application to the COVID-19 mortality rates. *Mathematics,* 10(7), Article 1015. https://doi.org/10.3390/math10071015

Aleshinloye, N. I., Aderoju, S. A., Abiodun, A. A., & Taiwo, B. L. (2023). A new generalized Gamma-Weibull distribution and its applications. *Al-Bahir Journal for Engineering and Pure Sciences,* 2(2), 92–100. https://doi.org/10.55810/2312-5721.1021

Alnaji, L., & Alghamdi, A. S. (2023). The exponentiated new Exponential-Gamma distribution: Properties and applications. *International Journal of Advanced and Applied Sciences*, 10(6), 71–79.

Ekhosuehi, N., Opone, F., & Odobaire, F. (2018). A new generalized two-parameter Lindley distribution. *Journal of Data Science*, 16(3), 549–566. https://doi.org/10.6339/JDS.201807_16(3).0006

Elangovan, R., Manivasagan, K., & Gijo, E. V. (2023). A new generalization of Samade distribution with properties and its applications in medical sciences. *Strad Research*, 10(6), 452–466.

Everitt, B. S., & Hand, D. J. (1981). Mixtures of normal distributions. In Finite Mixture Distributions (*Monographs on Applied Probability and Statistics*, pp. 25–57). Springer. https://doi.org/10.1007/978-94-009-5897-5_2

Fayomi, A., Khan, S., Tahir, M. H., Algarni, A., Jamal, F., & Abu-Shanab, R. (2024). Correction: A new extended Gumbel distribution: Properties and application. *PLoS ONE,* 19(8), e0309768. https://doi.org/10.1371/journal.pone.0309768

Gupta, R. D., & Kundu, D. (2001). Exponentiated exponential family: An alternative to Gamma and Weibull distributions. *Biometrical Journal*, 43(1), 117–130. https://doi.org/10.1002/1521-4036(200102)43:1<117::AID-BIMJ117>3.0.CO;2-R

Ibeh, G. C., Ekpenyoung, E. J., Anyiam, K., & John, C. (2021). The Weibull-exponential (Rayleigh) distribution: Theory and applications. *Earthline Journal of Mathematical Sciences, 6(1), 65–86.*

Idika, E. O., Ohakwe, J., Osu, B. O., & Onyemachi, C. U. (2021). α-Power transformed power function distribution with applications. *Heliyon,* 7(9). https://doi.org/10.1016/j.heliyon.2021.e08047

Lindley, D.V. (1958) "Fiducial distributions and Bayes' theorem," J. R. Stat. Soc. Ser. B, vol. 20, pp. 102–107. doi:10.1111/j.2517-6161.1958.tb00278.x.

Nadarajah, S., Bakouch, H. S., & Tahmasbi, R. (2011). A generalized Lindley distribution. *Sankhya B, 73*(3), 331–359. https://doi.org/10.1007/s13571-011-0025-9

Ogunwale, O. D., Adewusi, O. A., & Ayeni, T. M. (2019). Exponential-Gamma distribution. *International Journal of Emerging Technology and Advanced Engineering*, 9(10), 245–249.

Proloy, B., & Shreya, B. (2022). Exponential transformed inverse Rayleigh distribution: Statistical properties and different methods of estimation. *Austrian Journal of Statistics,* 51(4), 60–75. http://www.ajs.or.at/doi:10.17713/ajs.v51i4.1338

Qayoom, D., Rather, A. A., Alqasem, O. A., Ahmad, Z., Nagy, M., Yousuf,A.M., Mansi, A.H., Hussam, E. and Gemeay, A.M. (2025). Development of a novel extension of the Rayleigh distribution with application to COVID-19 data. *Scientific Reports*, 15, Article 18535. https://doi.org/10.1038/s41598-025-03645-w

R Core Team. (2025). R: A language and environment for statistical computing. R Foundation for Statistical Computing. https://www.r-project.org/

Suleman, I., Zakariyau, N. R., Oyegoke, O. A., Yahya, W. B., Amiru, F. M., & Umar, M. A. (2025). Notes on a modified Exponential-Gamma distribution: Its properties and applications. *Journal of Basics and Applied Sciences Research,* 3(2), Article 2. https://doi.org/10.4314/jobasr.v3i2.2

Thomas, B., & Chacko, V. M. (2022). Power generalized DUS transformation of exponential distribution. *International Journal of Statistics and Reliability Engineering*, 9(1), 150–157.

Umar, M. A., & Yahya, W. B. (2021). A new Exponential-Gamma distribution with applications. *Journal of Modern Applied Statistical Methods*. Retrieved from https://digitalcommons.wayne.edu/jmasm/about.html

Wang, J., Tian, L., & Yan, L. (2024). Statistical methods for comparing two independent Exponential-Gamma means with application to single-cell protein data. *PLoS ONE*, 19(12), e0314705. https://doi.org/10.1371/journal.pone.0314705